High-pressure elastic properties of liquid and solid neon to 7 GPa

Hiroyasu Shimizu,[1,2,*] Hiroki Imaeda,[2] Tetsuji Kume,[1] and Shigeo Sasaki[1,2]
[1]*Department of Materials Science and Technology, Gifu University, 1-1 Yanagido, Gifu 501-1193, Japan*
[2]*Environmental and Renewable Energy Systems, Graduate School of Engineering, Gifu University, 1-1 Yanagido, Gifu 501-1193, Japan*
(Received 8 September 2004; published 14 January 2005)

By using *in situ* high-pressure Brillouin spectroscopy in a diamond-anvil cell, we have determined the pressure dependence of acoustic velocities, adiabatic elastic moduli, bulk modulus, and elastic anisotropy of liquid and solid neon at pressures up to 7 GPa and 296 K through its liquid-solid phase transition point at 4.6 GPa. We investigate the characteristics of high-pressure elastic properties of the rare-gas solid neon by comparing to previous experiments of heavier elements, argon and krypton, and with recent theoretical calculations.

DOI: 10.1103/PhysRevB.71.014108 PACS number(s): 62.50.+p, 62.65.+k, 64.70.Kb, 78.35.+c

I. INTRODUCTION

Rare-gas solids (RGSs) are model substances that provide us with ideal systems allowing fruitful comparisons between experiments and theoretical calculations.[1] RGSs under high pressures are of fundamental interest as the hydrostatic pressure medium for high-pressure research in a diamond-anvil cell (DAC)[2,3] and as a component in rocks and the Earth's interior.[4] In our context of RGSs, solid helium is an extreme case where the quantum effect is very important. For the heavier RGSs argon, krypton, and xenon, the contributions from quantum motion of the atoms are not so strong. Therefore, solid neon is one of the most interesting among RGSs because its properties are expected to be intermediate between solid helium and the heavier elements.

High-pressure Brillouin spectroscopy is a useful method to study the elastic properties of molecular single crystals grown in the DAC.[5–7] By analyzing the observed angular dependence of Brillouin frequency shifts, acoustic velocities (v) for any direction, the refractive index (n), adiabatic elastic constants (C_{ij}), and adiabatic bulk modulus (B_S) can be exactly determined by Brillouin scattering measurements with *in situ* identification of the crystal orientation at each pressure. These results provide constraint on the forces of interaction between atoms or molecules at high compressions.[8,9]

At ambient pressure, neon (Ne) solidifies in the face-centered cubic (fcc) phase at about 24.4 K. At room temperature, liquid Ne crystallizes into the same phase at about 4.7 GPa,[10–12] and this pressure value is larger than 1.3, 0.83, and 0.42 GPa for those of Ar, Kr, and Xe, respectively.[1] Here, the helium shows its largest value of 11.5 GPa.[1,12,13] McLaren *et al.*[14] determined the adiabatic elastic constants of solid Ne at low temperatures and ambient pressure by Brillouin scattering measurements. By x-ray diffraction experiments at room temperature, Finger *et al.*[10] and Hemley *et al.*[15] determined the structure, lattice parameter, and *P-V* equation of state at pressures up to 14.4 GPa and 110 GPa, respectively. No solid–solid phase transition was observed to 110 GPa at room temperature. Hemley *et al.* also performed quasiharmonic lattice dynamics calculations for various pair-potential models of the solid.[15]

Recently, Tsuchiya and Kawamura[16] have calculated systematically elastic properties and their pressure dependence of RGSs up to $P=90$ GPa using the *ab initio* full-potential linear muffin-tin-orbital method. They have considered the Cauchy deviation, elastic anisotropy, and normalized elastic constants of Ne, Ar, Kr, and Xe solids as a function of pressure.

In this paper, we present acoustic velocities for all directions, deriving the refractive index, three adiabatic elastic constants (C_{11}, C_{12}, and C_{44}), adiabatic bulk modulus, elastic anisotropy, and normalized elastic constants of liquid and solid Ne at pressures up to 7 GPa. These properties were determined by using Brillouin scattering measurements with *in situ* identification of the crystal orientation[5–7] at each pressure. From these results we investigate the characteristics of high-pressure elastic properties for solid Ne by comparing with previous experiments of the heavier argon[8,17] and krypton,[18] and with recent theoretical calculations.[16]

II. EXPERIMENTAL AND ANALYSIS

For loading a Ne sample in the DAC, we pressurized commercial gaseous Ne at room temperature in a high-pressure gas vessel, including the DAC with an empty gasket hole, and sealed its fluid Ne in the sample chamber of the DAC. A single crystalline Ne was grown by increasing the pressure on a seed crystal, which coexists with the liquid Ne at $P=4.6$ GPa and 296 K. This pressure is close to the value reported previously.[10–12] The structure of the crystalline Ne is the fcc, but it does not show the crystal habit in the DAC. No pressure-transmitting medium was used because solid Ne is a soft material. Although the Ne crystal was occasionally strained on account of its softness, we could observe good Brillouin scattering signals under the condition of negligible nonhydrostatic stress at pressures up to 7 GPa. The pressure was measured by the ruby-scale method.[19] To minimize the effect of the pressure gradients in the Ne sample across the anvil, we used a tightly focused laser spot less than 10 μm, which is smaller than the sample size of about 100 μm. The 514.5 nm argon-ion laser line (λ_0) with a single longitudinal mode was used at input power of about 100 mW. The heart

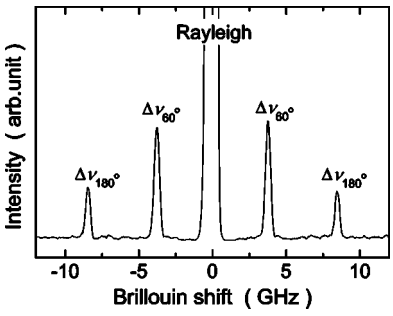

FIG. 1. Brillouin spectrum of liquid Ne at $P=1.28$ GPa. $\Delta\nu_{60°}$ and $\Delta\nu_{180°}$ are Brillouin-shifted signals from 60° and 180° scatterings, respectively.

of the apparatus was a Sandercock tandem Fabry–Perot interferometer,[20] which was used in a triple-pass arrangement. The Brillouin frequency shifts ($\Delta\nu$) at 60° and 180° scattering geometries with the DAC (angles between incident and scattered beams) are related to the acoustic velocity (v) as follows:[6,7]

$$\Delta\nu_{60°} = v_{60°}/\lambda_0 \tag{1}$$

and

$$\Delta\nu_{180°} = (2n)v_{180°}/\lambda_0, \tag{2}$$

where the wave vector q of the acoustic phonons is parallel (60°) and perpendicular (180°) to the interfaces of the input and output diamonds crossed by the laser beam, and $v_{60°}$ is independent of the refractive index of the medium. For the single crystalline Ne at pressures between 4.6 and 7 GPa, the elastic properties have been studied by using the method of *in situ* Brillouin spectroscopy developed for simple molecular solids.[5–7] The acoustic velocities can be calculated theoretically by using the above relation between $\Delta\nu$ and v, and the solution of the elastic equation as follows:[5–7]

$$v_j = f_j(C_{11}/\rho, C_{12}/\rho, C_{44}/\rho, \theta, \phi, \chi), \tag{3}$$

where the subscript j (=0,1,2) indicates the longitudinal acoustic (LA), two transverse acoustic TA_1(slow), and TA_2(fast) modes, respectively, and the Euler angles (θ, ϕ, χ) indicate the crystal orientation in the DAC. In order to determine the three Euler angles and three elastic constants simultaneously at each pressure, we applied a computerized least-squares fit between the calculated $f_j(\phi_i)$ and experimental acoustic velocities (ϕ_i, v_{ij}) as a function of angle ϕ_i

$$J = \sum_{ij} [f_j(\phi_i) - v_{ij}]^2, \tag{4}$$

where $j=0$, 1, 2, and the sum of square errors is minimized by systematically varying the six parameters until the fit is optimized. As a result, we can determine a complete mapping of the acoustic velocities in the various crystal directions with *in situ* identification of the crystal orientation.[5–7]

III. RESULTS AND DISCUSSION

We determined the pressure dependence of acoustic velocities and the refractive index for liquid Ne at pressures up

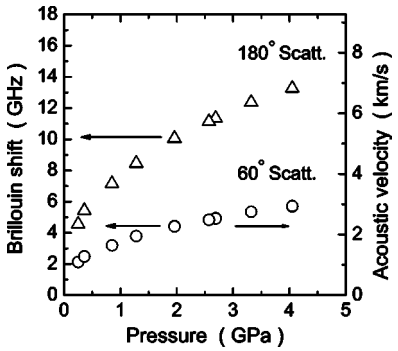

FIG. 2. Pressure dependence of Brillouin frequency shifts at 60° and 180° scatterings for liquid Ne. Open circles (60° scattering) indicate acoustic velocity simultaneously.

to 4.6 GPa and 296 K. A typical Brillouin spectrum of liquid Ne ($P=1.28$ GPa) at 60° scattering geometry is shown in Fig. 1. We can observe Brillouin frequency shifts for $\Delta\nu_{60°}$ and $\Delta\nu_{180°}$, simultaneously, because the laser beam reflected from the output diamond serves as an incident beam, giving the weak 180° scattering signal.[21,22] Figure 2 shows the pressure dependence of $\Delta\nu_{60°}$, $\Delta\nu_{180°}$, and the sound velocity ($v_{60°}$) from Eq. (1) below $P=4.6$ GPa. Because the liquid is acoustically isotropic, the sound velocity is the same for all directions. Therefore, we can determine the pressure dependence of n by using Eqs. (1) and (2); that is, the ratio of $\Delta\nu_{60°}$ to $\Delta\nu_{180°}$ and $\Delta\nu_{60°}/\Delta\nu_{180°}=1/(2n)$ (see open circles in Fig. 3). The refractive index increases sharply with pressure and has, near the solidification point, a value of about 1.16, which is lower than that of H_2O at $P=0.1$ MPa and room temperature. The present results are in good agreement with those of Dewaele *et al.*[12] by the interference method within the error of ±1 % (see Fig. 3). For solid Ne at pressures between 4.6 and 7 GPa, the acoustic and elastic properties have been studied by using the method of *in situ* high-pressure Brillouin spectroscopy mentioned above. A typical Brillouin spectrum of solid Ne at 6.09 GPa is shown in Fig. 4. The peaks of LA and TA modes are clearly observed. The signal from TA (shear) modes looks like one peak, whereas two peaks are usually expected to appear, except for the

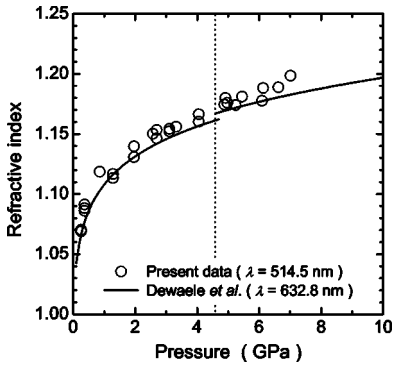

FIG. 3. Pressure dependence of the refractive index (n) for liquid and solid Ne (open circles) at 296 K. The vertical dashed line indicates the liquid-solid phase transition point at $P=4.6$ GPa. The solid line shows the recent results of the interference method by Dewaele *et al.*[12]

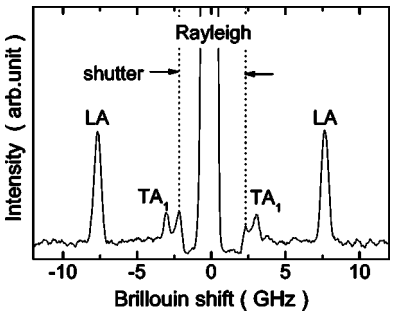

FIG. 4. Brillouin spectrum of solid Ne at $P=6.09$ GPa. LA and TA_1 are Brillouin-shifted signals from longitudinal and slow transverse modes, respectively. The shutter works to attenuate the strong Rayleigh intensity when scanning through its peak.

cases of (i) the weak intensity for one of their peaks; (ii) nearly elastic isotropy, i.e., the close frequencies of two shear modes;[23] and (iii) the phonon wave vector along the ⟨100⟩ or ⟨111⟩ direction in a cubic system. By considering the previous results of Brillouin measurements at low temperature and ambient pressure[14] that showed one TA_1 peak and the elastic anisotropy, in the present only one peak appeared for TA modes, which is probably due to the weak intensity of TA_2 peak. This prediction can be confirmed reasonably by the following fitting method between the calculation and the measured values of acoustic velocities. Brillouin measurements at 60° scattering geometry were made in 10° intervals of rotation angle ϕ about the load axis of the DAC in the laboratory frame. The observed Brillouin frequency shifts, that is, acoustic velocities at 5.24 GPa, are plotted as a function of ϕ by open circles in Fig. 5. By using Eqs. (3) and (4) the computerized least-squares fit was applied to determine (i) whether the observed TA mode corresponds to TA_1 or TA_2, and as a result, (ii) acoustic velocities and elastic constants of the fcc Ne single crystal at each pressure. For the case of assuming TA_2 mode observed, the fitting could not be optimized at all. For another case of TA_1 mode, we found excellent agreement between the measured and the fitted values, as seen in Fig. 5. Therefore, the observed TA mode could be consistently confirmed to be TA_1. The best fitting results yielded $C_{11}/\rho=11.50$, $C_{12}/\rho=9.69$, and $C_{44}/\rho=4.27$ km^2/s^2, and $\theta=54.9°$ and $\chi=12.4°$ at $P=5.24$ GPa.

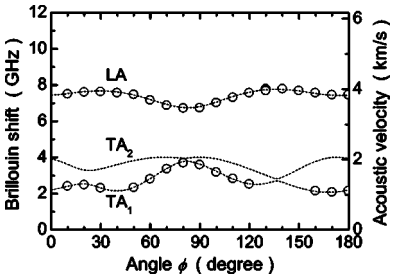

FIG. 5. Brillouin frequency shifts and acoustic velocities of LA, TA_2, and TA_1 modes as a function of angle ϕ at a 60° scattering geometry for solid Ne at $P=5.24$ GPa. The ϕ shows the rotation angle about the load axis of DAC. Open circles indicate experimental points, and dashed lines represent the calculated best-fit velocities.

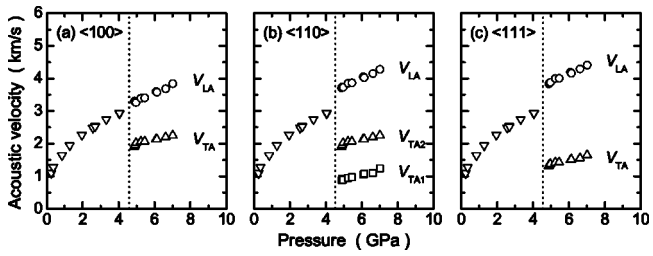

FIG. 6. Pressure dependence of acoustic velocities for liquid and solid Ne at 296 K. The vertical dashed line indicates the liquid-solid phase transition point at $P=4.6$ GPa. In the fcc solid phase, the velocities for typical directions are shown: (a) ⟨100⟩, (b) ⟨110⟩, and (c) ⟨111⟩ directions. LA, TA_2, and TA_1 are longitudinal, fast, and slow transverse modes, respectively.

Once the six parameters were determined, the acoustic velocities including TA_2 mode could be calculated for all directions. Figure 6 shows the Ne acoustic velocities for typical directions as a function of pressure up to 7 GPa at 296 K. At the freezing point (=4.6 GPa), the acoustic velocity shows a discontinuous change to the LA, TA_2, and TA_1 velocities in the solid phase of Ne, and these increase with pressure. Furthermore, we can calculate the acoustic velocity ($v_{180°}$) along the direction perpendicular to the diamond interfaces, which allows us to determine the refractive index (n) by using Eq. (2). From the $\Delta\nu_{180°}$ measured at 180° scattering geometry, we can obtain the pressure dependence of n as shown in Fig. 3. The refractive index is almost continuous across the freezing point, probably due to the van der Waals solid being a simple closed-shell insulator. The n of solid Ne shows a gradual increase with pressure. The present result is in good agreement with those obtained by Dewaele *et al.*[12] In Fig. 7(a) we show the pressure dependence of the three C_{11}, C_{12}, and C_{44} of Ne by open symbols, which were determined from the best-fitted results for C_{ij}/ρ with the pressure dependence of ρ from x-ray studies.[10,15] Typical values at $P=6$ GPa and 296 K are as follows: $C_{11}=34.9$, $C_{12}=28.7$,

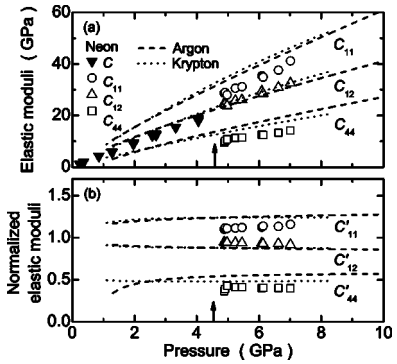

FIG. 7. (a) Pressure dependence of adiabatic elastic constants, C_{11}, C_{12}, and C_{44} for solid Ne at 296 K (open symbols). For the liquid phase (solid symbol), the elastic modulus is $C=\rho v^2$. The vertical arrow indicates the liquid–solid phase transition point at $P=4.6$ GPa. Adiabatic elastic constants of pressure-induced crystalline Ar[8] and Kr[18] are shown for comparison by broken and dashed lines, respectively. (b) Normalized adiabatic elastic constants $C'_{ij}(=C_{ij}/B_S)$ of crystalline Ne, Ar, and Kr at room temperature.

C_{44}=12.4 GPa, and deriving B_S [=$(C_{11}+2C_{12})/3$] =30.8 GPa. These values cannot be compared to those of low-temperature solid Ne because its C_{12} and C_{44} changed drastically around T=16 K.[14] Furthermore, the previous results of Ar[8,17] and Kr[18] are also presented by respective broken and dashed lines for comparison. The C_{12} of solid Ne shows almost the same value as those of solids Ar and Kr, but C_{11} and C_{44} clearly indicate the lower values than those of Ar and Kr at respective pressures. The agreement of the present Ne data with the recent theoretical calculation[16] is not so good because first-principles calculations do not contain the van der Waals forces effective at lower pressures. Therefore, the present results will provide experimental verification to ground the calculation in reality. On the other hand, the pressure dependences of experimental C_{ij}, dC_{11}/dP=5.9, dC_{12}/dP=4.1, and dC_{44}/dP=2.0 are in good agreement with those values of theoretical calculations, 5.7, 4.0, and 2.4.[16]

Tsuchiya and Kawamura[16] investigated the elasticity of RGSs by using the normalized elastic constants $C'_{ij}=C_{ij}/B_S$, which are obtained by dividing the specific elastic constant with the bulk modulus.[24] Dividing by the bulk modulus, the interatomic forces are considered to be normalized with an average restoring force of the system. If a cubic crystal is ideal, that is, the isotropic Cauchy solid, then 1.8, 0.6, and 0.6 are found for C'_{11}, C'_{12}, and C'_{44} at zero pressure, respectively.[16] Their calculation indicated that C'_{ij} of RGSs are quite insensitive to pressure, and although the dependence of C'_{ij} on the RG element is small, C'_{11} and C'_{44} of Ne show the lowest values and C'_{12} does the highest one. In Fig. 7(b) the pressure dependence of our experimental C'_{ij} for Ne, Ar, and Kr solids are presented. The present C'_{11} and C'_{44} of Ne are lower than those of Ar and Kr, and C'_{12} is higher than that of Ar and Kr, which are similar to the results of theoretical investigation.[16] These characteristics of solid Ne clearly indicate the different properties from the heavier RGSs.

A measure of the elastic anisotropy is given by $A=2C_{44}/(C_{11}-C_{12})$ for cubic crystals.[5] For isotropic elasticity, the two shear moduli C_{44} and $(C_{11}-C_{12})/2$ are equal and A=1. Figure 8 compares the pressure dependence of A for solid Ne with those of Ar and Kr solids. The behavior of Ne is remarkable; that is, a large value of A=4.89 at 5 GPa shows a rapid decrease to 3.62 at 7 GPa. These properties cannot be compared to theoretical calculation because of no result at this low-pressure range. However, it is noted that the calculated A of Ne is the largest among RGSs, and A=4 around P=10 GPa.[16] Furthermore, as for the Cauchy violation $\delta=C_{12}-C_{44}-2P$, the present experiment of solid Ne shows about δ=5 and almost constant at pressures between 4.6 and 7 GPa. We cannot discuss about this δ in more detail because of its narrow pressure range.

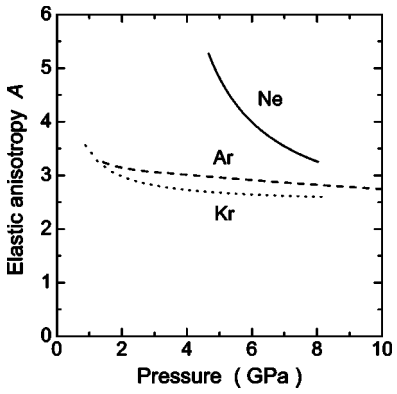

FIG. 8. Pressure dependence of elastic anisotropy A [=$2C_{44}/(C_{11}-C_{12})$] for pressure-induced crystalline Ne, Ar, and Kr at room temperature.

At last we estimate the pressure dependence of the ratio of specific heats, $\gamma=C_P/C_V=B_S/B_T$, where the adiabatic bulk modulus B_S [=$(C_{11}+2C_{12})/3$] is determined from the present Brillouin results and the isothermal bulk modulus B_T [=$\rho(dP/d\rho)_T$] from x-ray studies.[5–8] The value of γ shows 1.32 at P=4.9 GPa and decreases to 1.18 at 7.0 GPa with increasing pressure. This behavior is reasonable for RGSs.[8,18,25]

IV. SUMMARY

We have determined high-pressure elastic properties of liquid and solid Ne up to 7 GPa at room temperature by using *in situ* Brillouin spectroscopy with a diamond-anvil cell. These were compared with previous experiments of heavier Ar and Kr and with recent theoretical calculations. The present C_{12} of solid Ne shows almost the same value as those of solids Ar and Kr, but C_{11} and C_{44} clearly indicate the lower values than those of Ar and Kr at respective pressures. The normalized elastic constants $C'_{ij}=C_{ij}/B_S$ of crystalline Ar and Kr show almost the same values. The present C'_{11} and C'_{44} of Ne are lower than those of Ar and Kr, and C'_{12} is higher than that of Ar and Kr, which are similar to the results of theoretical investigation. These characteristics of solid Ne clearly indicate the different properties from the heavier RGSs.

*Electronic address: shimizu@cc.gifu-u.ac.jp

[1] *Rare Gas Solids*, edited by J. A. Venables and M. L. Klein (Academic, New York, 1976), Vols. I and II.
[2] P. M. Bell and H. K. Mao, Year Book - Carnegie Inst. Washington **80**, 404 (1981).
[3] K. Takemura, J. Appl. Phys. **89**, 662 (2001).
[4] A. P. Jephcoat, Nature (London) **393**, 355 (1998).
[5] H. Shimizu and S. Sasaki, Science **257**, 514 (1992).
[6] H. Shimizu, in *High Pressure Research on Solids*, edited by M. Senoo, K. Suito, T. Kobayashi, and H. Kubota (Elsevier Science, The Netherlands, 1995), pp. 1–17.
[7] H. Shimizu, T. Nabetani, T. Nishiba, and S. Sasaki, Phys. Rev. B **53**, 6107 (1996).
[8] H. Shimizu, H. Tashiro, T. Kume, and S. Sasaki, Phys. Rev. Lett.

86, 4568 (2001).
[9] A. Polian, J. Raman Spectrosc. **34**, 633 (2003).
[10] L. W. Finger, R. M. Hazen, G. Zou, H. K. Mao, and P. M. Bell, Appl. Phys. Lett. **39**, 892 (1981).
[11] W. L. Vos, J. A. Schouten, D. A. Young, and M. Ross, J. Chem. Phys. **94**, 3835 (1991).
[12] A. Dewaele, J. H. Eggert, P. Loubeyre, and R. Le Toullec, Phys. Rev. B **67**, 094112 (2003).
[13] A. Polian and M. Grimsditch, Europhys. Lett. **2**, 849 (1986).
[14] R. A. McLaren, H. Kiefte, D. Landheer, and B. P. Stoicheff, Phys. Rev. B **11**, 1705 (1975).
[15] R. J. Hemley, C. S. Zha, A. P. Jephcoat, H. K. Mao, L. W. Finger, and D. E. Cox, Phys. Rev. B **39**, 11 820 (1989).
[16] T. Tsuchiya and K. Kawamura, J. Chem. Phys. **117**, 5859 (2002).
[17] H. Shimizu, J. Phys.: Condens. Matter **14**, 10 657 (2002).
[18] H. Shimizu, N. Saitoh, and S. Sasaki, Phys. Rev. B **57**, 230 (1998).
[19] F. D. Barnett, S. Block, and G. J. Piermarini, Rev. Sci. Instrum. **44**, 1 (1973).
[20] R. Mock, B. Hillebrands, and R. Sandercock, J. Phys. E **20**, 656 (1987).
[21] H. Shimizu, E. M. Brody, H. K. Mao, and P. M. Bell, Phys. Rev. Lett. **47**, 128 (1981).
[22] E. M. Brody, H. Shimizu, H. K. Mao, P. M. Bell, and W. A. Bassett, J. Appl. Phys. **52**, 3583 (1981).
[23] H. Shimizu, T. Kumazaki, T. Kume, and S. Sasaki, Phys. Rev. B **65**, 212102 (2002).
[24] L. Fast, J. M. Wills, B. Johansson, and O. Eriksson, Phys. Rev. B **51**, 17 431 (1995).
[25] A. I. Karasevskii and W. B. Holzapfel, Phys. Rev. B **67**, 224301 (2003).